Journal of Solid State Chemistry **155,** 154–167 (2000)
doi:10.1006/jssc.2000.8916, available online at http://www.idealibrary.com on IDEAL®

On the Various Approaches to Enhancing the Conductivity of Sodium Sulfate: Review and Current Developments

Prakash Gopalan,[1] Sandeep Saha, Santosh Bobade, and Ajit Kulkarni

Department of Metallurgical Engineering and Materials Science, IIT Powai, Mumbai 400 076, India

Received June 26, 2000; in revised form July 28, 2000; accepted August 2, 2000

DEDICATED TO PROFESSOR J. M. HONIG

The various approaches to enhancing the conductivity of Na_2SO_4 are reviewed. The role of the size of the dopant cation on the conductivity enhancement has been emphasized. As for anion doping, apart from the size, the role of the shape and orientational ordering of the dopant ion has been highlighted. The structure of the guest ion appears to influence the stabilization of Na_2SO_4–I at low temperatures. A recent development has been the formation of Na_2SO_4-based composites. In this work, the stabilization of the Na_2SO_4–I phase for the 4 m/o $La_2(SO_4)_3$ composition in the Na_2SO_4–$La_2(SO_4)_3$ system has been established at 120°C through structural evidence. Several new features appear in the conductivity behavior of the Na_2SO_4–Al_2O_3 composite system. In contrast to a previous study, we now observe and report the formation of the high conducting Na β-alumina phase for the 5 m/o Al_2O_3 composition. As before, two peaks are observed in the conductivity–composition plot, a feature not commonly encountered in known composite systems. Unlike other composite electrolyte systems, the size of the dispersoid phase does not appear to affect the conductivity enhancement. Furthermore, in most known systems, γ-Al_2O_3 is used as a dispersoid. However, enhancements in conductivity for the Na_2SO_4–Al_2O_3 system have been observed only when the identified phase is α-Al_2O_3. © 2000 Academic Press

Key Words: **Na_2SO_4–Al_2O_3 system; phase stabilization; cation doping; anion doping; role of dopant size; Na β-alumina; nanoparticles.**

1. INTRODUCTION

Much has been discussed in literature on sulfate-based solid electrolytes. About 2 years ago, this point was reinforced by none other than the editor of a leading journal in this area of research, who used his discretion in turning down a manuscript, without even a peer review. His contention was that too much was being done, without substantially changing our understanding of the already known facts about these materials. Therefore, his journal, as a policy, would not publish a work unless the results or the interpretation substantially altered our present understanding about these materials. While one may agree or disagree with his discretion, it is true, and with reason, that a lot of interest still exists in these materials. However, no recent reviews on the electrical properties of pure and doped Na_2SO_4 are available.

The mechanism of conduction in alkali sulfates has been hotly debated (1–17), and the flurry of activities relating to development of a sulfate-based material with a large conductivity at or about room temperature still continues. A good stable electrolyte that can be used in a solid-state battery or in a SO_2/SO_3 gas sensor satisfactorily is yet to be developed. The main requirements of a solid electrolyte for application in SO_2/SO_3 gas sensing are that it should undergo reversible electrochemical reaction with SO_2/SO_3 and have minimum electronic conductivity. Alkali metal sulfates satisfy both these requirements and are therefore considered as good candidates for the SO_2 sensor. Table 1 lists the solid electrolytes that have been proposed for the detection of SO_2/SO_3 gases.

The alkali sulfates possess several advantages over other solid electrolytes, namely, their resistance to thermal decomposition, nonhygroscopic nature, and easy availability. Most sulfate systems such as Li_2SO_4, Na_2SO_4, Ag_2SO_4, $LiNaSO_4$, and $Li_{1.33}Zn_{0.33}SO_4$ attain high conductivity values at high temperatures after undergoing a first-order transition. However, the K, Rb, and Cs salts show much lower conductivity due to their relatively larger ionic size and are not considered promising solid electrolytes. Table 2 provides some relevant thermodynamic data for some fast conducting sulfates.

It is evident from the above data that Li, Na, and Ag ion conductors have distinct advantages over each other. Lithium ion conductors have the highest conductivity due to the small ionic radius and low atomic weight of Li. However, the phase transitions of most of these sulfates are difficult to suppress owing to their high heats of transformation. In

[1] To whom correspondence may be addressed. E-mail: pgopalan@met.iitb.ernet.in.

0022-4596/00 $35.00

TABLE 1
Solid Electrolytes used in SO_2/SO_3 Sensors

Sensor material	Dynamic range (concentration detection)	Temp. (°C)	Ref.
K_2SO_4	10 ppm–1%	820	18
$CaO–ZrO_2/K_2SO_4$	5 ppm–1%	780	19
$Na_2SO_4–Y_2(SO_4)_3–SiO_2$	200 ppm–20%	700	20
$NASICON/Na_2SO_4$	50 ppm–1%	780	21
$Na_2SO_4–La_2(SO_4)_3–Al_2O_3$	50 ppm–1%	700	22
$CaF_2/CaSO_4$	0.3 ppm–20%	630	23
$Na–\beta/\beta''–Al_2O_3/Na_2SO_4$	2 ppm–20%	500–900	24
$Ag_2SO_4–Li_2SO_4$	5 ppm–1%	700	25
$Ca–\beta/\beta''–Al_2O_3/CaSO_4$	2 ppm–20%	700	26
$MgO–ZrO_2/Li_2SO_4–CaSO_4$	20–200 ppm	700	27
$MgO–ZrO_2/Li_2SO_4–CaSO_4–SiO_2$	2–200 ppm	600–750	28

particular, the high-temperature rotator phases in Table 2, namely Li_2SO_4, $LiNaSO_4$, $LiAgSO_4$, and Li_4ZnSO_4, have a solid–solid transformation enthalpy higher than those observed for melting. The electrical conductivity of these rotator phases are comparable to those of a melt. In that sense, Na_2SO_4 and Ag_2SO_4 are different from those classified as belonging to the rotator phases. Of these, Ag_2SO_4 shows a reasonably good conductivity at lower temperatures but for many applications, the high cost of Ag becomes prohibitive.

The phase transitions in Na_2SO_4, leading to a high-conducting phase, occur at a temperature more than 300°C below that for Li_2SO_4 (Table 2). Thus, the Na^+ ion conductivity is much higher than any other fast ion-conducting sulfate between 250 and 500°C. Moreover, the heat of phase transformation also happens to be the lowest for Na_2SO_4. It has been, therefore, easier to attempt stabilizing the high-temperature phase of Na_2SO_4 by forming solid solutions with homovalent or aliovalent cations (20–22, 32–48) and/or anions (6, 49–59). In recent times, attempts have also been made to enhance the conductivity of Na_2SO_4 through composite formation (60). The main focus of most research initiatives has been directed at lowering the transition temperature and increasing the conductivity of Na_2SO_4.

TABLE 2
Relevant Thermodynamic Data of Some Sulfate Solid Electrolytes

Salt	T_t (°C)	ΔH_t (KJ/mol)	σ (S/cm) at 823 K	Q (σT) (eV)	Reference
Li_2SO_4[a]	575	24.8	0.86	0.43	29
$LiNaSO_4$[a]	518	24.7	0.93	0.44	10
$LiAgSO_4$[a]	455	34.3	1.17	0.40	30
$Li_{1.33}Zn_{0.33}SO_4$[a]	482	25.2	1.00	0.36	10
Na_2SO_4[b]	247	11.6	0.0007	0.47	31
Ag_2SO_4[b]	420	17.0	0.02	0.49	6

Note. T_t is the transition temperature; ΔH_t, the transition enthalpy; σ, the ionic conductivity; Q (σT), the activation energy from conductivity data.
[a] Rotator phases.
[b] Nonrotator phases.

In this work, the current status of development on Na_2SO_4-based materials and results of some of the known strategies adopted for enhancing the conductivity in our laboratory have been presented and discussed. These strategies have been classified as aliovalent cation doping, homovalent anion and cation doping, and composite formation. In light of the existing literature, areas that need to be addressed more critically have been identified. Following the literature reviewed below, a few of those identified areas have been investigated in this work.

2. LITERATURE REVIEW

Sodium sulfate exhibits five polymorphs between 200 and 235°C. Kracek and Gibson (61) have proposed the equilibrium scheme for the various phase transitions in Na_2SO_4. All the low-temperature forms have an orthorhombic crystal structure. Of these, only phases **I, III,** and **V** are stable and have been well characterized. The **III–I** phase transition results in a 4% volume expansion and exhibits a sharp jump by a factor of 10 in conductivity (31). The structure of the high-temperature form, Na_2SO_4–I, is hexagonal (space group $P6_3/mmc$) and consists of isolated SO_4 tetrahedra and two nonequivalent Na positions (41). It was pointed out that this form could be visualized as layers parallel to the *c*-axis, some containing only Na ions and others containing a mixture of Na and SO_4 ions. However, they clearly stated that the details of the defect structure are not clearly understood.

The defect structure in Na_2SO_4 remains unclear. In fact, the very question of whether Schottky or Frenkel types of defects prevail in Na_2SO_4 is still not answered. The general guidelines, based purely on the ionic radii of the cation and the anion, suggest that Na_2SO_4 is quite likely to exhibit cationic Frenkel defects (34, 35). There is no other sodium salt involving divalent anions with a known defect structure to substantiate the above proposition. It is ironic that in spite of the attention that this material has received, fundamental issues relating to structure and defect chemistry have still not been clearly understood.

Unlike Li_2SO_4, where the conduction mechanism has been hotly debated and still remains unresolved (7–17), it is now a widely accepted fact that the percolation-type transport mechanism of ions is responsible for the high Na^+ mobility in Na_2SO_4 (5). The percolation model proposes the existence of percolation pathways through a network of interconnected irregularly positioned sites with cation occupancy. It states that the ion transport in solids occurs by a process of activated hopping, as the ion surmounts the potential energy barrier of the neighboring sites. At the

phase transition, the number of interstice channel connectivities or the percolation probability in the network structure increases sharply. The transformation to the high-temperature disordered phase which is accomplished by lattice expansion ($\sim 4\%$ in Na_2SO_4) increases the freedom of cation movement and the number of accessible interconnected sites and thereby results in higher ionic conductivity.

However, Kvist *et al.* (2) proposed that the cooperative motion of cations and the anion-assisted movement of cations or the so-called "cogwheel" mechanism was responsible for the high cationic mobility and conductivity. To test this mechanism, Secco (3) incorporated the anions WO_4^{2-} and SiO_4^{4-} as guest ion in the Na_2SO_4 structure. The larger radius isovalent WO_4^{2-} with 2.5 times the mass of SO_4^{2-} would lower the conductivity if the cogwheel mechanism were operative. On the other hand, if a more open lattice structure due to simple lattice expansion contributes to the conductivity, then an increase in conductivity for the WO_4^{2-}-doped Na_2SO_4 was predicted. The SiO_4^{4-} anion possessing a mass equivalent to the mass of SO_4^{2-} can be accommodated by excess Na^+ generated on interstitial sites or by SO_4^{2-} vacancies that represent missing "cogwheels." This would lead to a lower conductivity on the basis of the cogwheel mechanism. On the other hand, SO_4^{2-} vacancies provide a more open network with greater freedom of motion which would result in an increase in conductivity. In each case, it was observed that the guest ion not only enhanced the conductivity by a factor of 10 but also lowered the transition temperature by 30°C. These results, according to Secco *et al*., conclusively showed that the cogwheel mechanism did not contribute to the high cation conductivity in Na_2SO_4. It must, however, be stressed here that similar attempts by Secco and coworkers (15) to explain the conductivity of Li_2SO_4 and $LiNaSO_4$ were largely unsuccessful. The results and the interpretations were contested strongly by researchers who believed that the conductivity in those systems could be explained on the basis of the paddle-wheel or the cogwheel mechanism alone (7–10). The basic premise on which the results were interpreted was dependent on whether the anion dopants had formed a solid solution with Li_2SO_4. Lunden *et al.* (7–10) have consistently claimed that the results and also the experimental techniques that Secco *et al.* reported were inadequate for the activity they had undertaken. It was also pointed out that the results reported by Secco *et al.* were in fact for two-phase mixtures, where a different mechanism is operative and could account for the increase observed in the conductivity. The reader is referred to a more balanced review of the subject (16). However, it appears that this debate on the mechanism of conductivity has still not been resolved and continues to date.

For pure Na_2SO_4, the general aspects relating to the crystal as well as defect structure and the conduction mechanism have been, thus far, reviewed. It is also known that the conductivity of Na_2SO_4 is highly sensitive to the presence of even small amounts of impurity (35). In order to lend a structure to this review, the existing literature on doped Na_2SO_4 has been divided into research involving hetero- and homovalent cationic substitution, anionic substitution, and composite formation.

A. Cation Substitution in Na_2SO_4

Following the work of Keester *et al.* (32), who reported that Na_2SO_4 forms extended solid solubility with other di- and trivalent sulfates, resulting in as much as 30 mol% vacancy concentration, many workers have tried to enhance the conductivity and/or stabilize the Na_2SO_4–I phase to lower temperatures. The work of Keester *et al.* can therefore be considered as being a pioneering one as far as cation substitution in Na_2SO_4 is concerned. They showed that in the Na_2SO_4–$MeSO_4$ systems (Me = Ni, Mg, Cu, Co, Zn, Mn, Cd, Ca, Sr, Pb, Ba), extended solid solutions for Na_2SO_4–I occur with cation substitutions and also that it is possible to incorporate trivalent ions (Fe, In, Y, Gd, La).

Hofer *et al.* (33) studied the conductivity behavior of the Na_2SO_4–I solid solutions formed by the aliovalent cations- Zn^{2+}, Ni^{2+}, Sr^{2+}, and Y^{3+}. They reported the presence of a maximum in conductivity at 7% vacancy concentration in all the solid solutions, *irrespective of the size, charge, or nature of the substituting cations*. Hofer *et al.* also reported that doping $Y_2(SO_4)_3$ into Na_2SO_4 stabilizes the high-temperature phase and increases the electrical conductivity. Following this, Saito *et al.* (39, 40) studied the phase transition and electrical properties of this system. They reported that an addition of yttrium less than 1.7 at.% lowered the transition temperature to $\cong 170$°C and the maximum conductivity of 1.6×10^{-1} $(\Omega\,\mathrm{cm})^{-1}$ was obtained in the sample containing 3.8 at.% Y at 800°C. In order to prevent the electrolyte from being ductile and to achieve further enhancement in conductivity, Imanaka *et al.* doped this system with sodium vandate (47), silicon dioxide (20), and alumina (20). The Na_2SO_4–$NaVO_3$–$Y_2(SO_4)$ system maintained the high temperature phase Na_2SO_4–I, without exhibiting any phase transformations. However, this electrolyte could not be used at temperatures higher than 450°C. The problem was overcome by the same workers by mixing alumina in the Na_2SO_4–$La_2(SO_4)_3$ system so as to obtain a harder and heat durable electrolyte (22). This mixture exhibited 30 times larger conductivity at 700°C, and proved to be a better SO_2 sensor.

Rao *et al.* (38) showed that compositions containing 12 or more m/o $Y_2(SO_4)_3$ in the Na_2SO_4–$Y_2(SO_4)_3$ systems can completely stabilize the Na_2SO_4–I structure at room temperature. To the solid electrolyte containing 5 m/o $Y_2(SO_4)_3$, 5–20 m/o Na_2WO_4 was added in order to improve both the stability of phase I, as well as the mechanical behavior of the electrolyte.

The effect of many other rare-earth ions on the phase transition in Na_2SO_4 has been widely investigated by several workers (20, 33–40, 48), the reason being that Na_2SO_4 doped with $Ln_2(SO)_3$ (Ln = Y, Eu, Pr, La, Dy, Sm, Tm) shows high conductivity and maintains phase I without exhibiting any phase transformation.

Shahi and coworkers (34, 35) have attributed the high conductivity of rare-earth (La^{3+}, Sm^{3+}, Dy^{3+}, and Im^{3+})-doped Na_2SO_4 systems to the excess of Na^+ vacancies created as a result of replacing Na^+ with Ln^{3+} ions in the Na_2SO_4 lattice. An examination of the conductivity enhancements versus size of various trivalent ions showed that the conductivity enhancement is favored when the ionic radius of the dopant is close to that of host sodium ion. The highest conductivity value obtained in the Na_2SO_4–$La_2(SO_4)_3$ system was $1.08 \times 10^{-3}\ \Omega^{-1}\,cm^{-1}$ at 290°C, namely, only an order of magnitude less than the best Na^+ conductors available.

As in the case of Na_2SO_4–$Y_2(SO4)_3$ electrolytes, Imanaka *et al.* (47) showed that the electrical conductivity of sodium sulfate doped with rare-earth sulfates improved on the addition of $NaVO_3$.

Bandarnayake *et al.* reported the phase transition behavior of the Na_2SO_4–$MgSO_4$ (45) and Na_2SO_4–$CaSO_4$ (46) systems. In both cases, only an enhancement in conductivity at high temperatures was observed.

In spite of a large number of investigations on cationic substitution in Na_2SO_4, until about 2 years ago, the understanding of the relationship between dopant size and conductivity appeared limited to extreme and contradictory views (33, 35, 42). It is fair to state that neither of the opposing views was based on studies involving a large number of binary systems. This prompted Singhvi *et al.* (48) to investigate the role of the size and nature of the dopant on the conductivity of Na_2SO_4. Singhvi *et al.* chose eight cations with significantly different sizes. The dopants used were sulfates of Ba^{2+} (1.36 Å), Sr^{2+} (1.16 Å), La^{3+} (1.06 Å), Nd^{3+} (1.00 Å), Sm^{3+} (0.96 Å), Y^{3+} (0.89 Å), Ce^{4+} (0.80 Å), and Zr^{4+} (0.72 Å). The choice of the cations had been dictated by the size of Na^+ (1.02 Å), taken from the compilation of Shannon and Prewitt (62). Their results are discussed below in some detail.

In Fig. 1, the DSC plots for the 2 m/o compositions of various cations show that the peak at 241°C in pure Na_2SO_4 is pretty much present around the same temperature for the doped compositions. For the 2 m/o Ba^{2+} composition the peaks at 256°C, and for the Sr^{2+}-doped composition those at 210 and 246°C, have been interpreted to be corresponding to the **V–I**, and the **V–III–I** transitions, respectively. However, it is not always possible to associate the peaks around 200°C to phase transitions in Na_2SO_4. This is best illustrated in the case of the 2 m/o Y^{3+} and the La^{3+}- doped compositions. For example, in the DSC curves in Fig. 1, one would be tempted to associate the peak for the

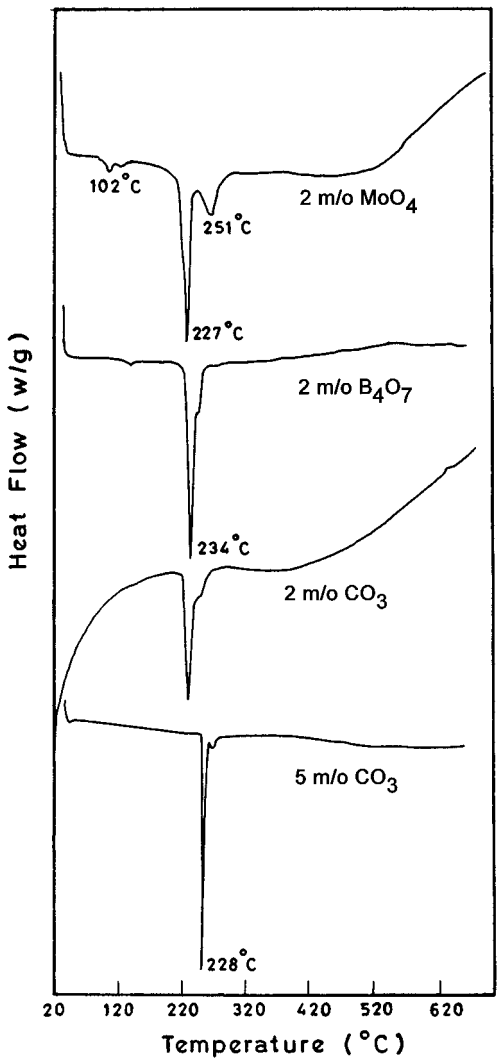

FIG. 1. DSC traces for the 2 m/o anion-doped Na_2SO_4 compositions.

2 m/o $La_2(SO_4)_3$ and the 2 m/o $Y_2(SO_4)_3$ composition to the **V–I** phase transition in Na_2SO_4. On the other hand, the conductivity results for the 2 and 4 m/o $La_2(SO_4)_3$ compositions in Fig. 2a and those for the $Sm_2(SO_4)_3$-doped systems in Fig. 2b show that the Na_2SO_4–I phase persists well below 100°C. This inference has been drawn by the fact that the slope of the log σ vs $10^3/T$ plot, a measure of the activation energy, remains unchanged. A phase transition would have ensured a change in the activation energy, with the slopes being different for the two phases. Singhvi *et al.* have shown similar log σ vs $10^3/T$ plot for the 2 m/o $Y_2(SO_4)_3$ composition as well. As a consequence, differences are likely between the DSC and conductivity results, unless the DSC peaks can be identified with thermal events unrelated to phase transitions in Na_2SO_4. To make the DSC data consistent with the conductivity, it would be better to substantiate the findings through high-temperature XRD.

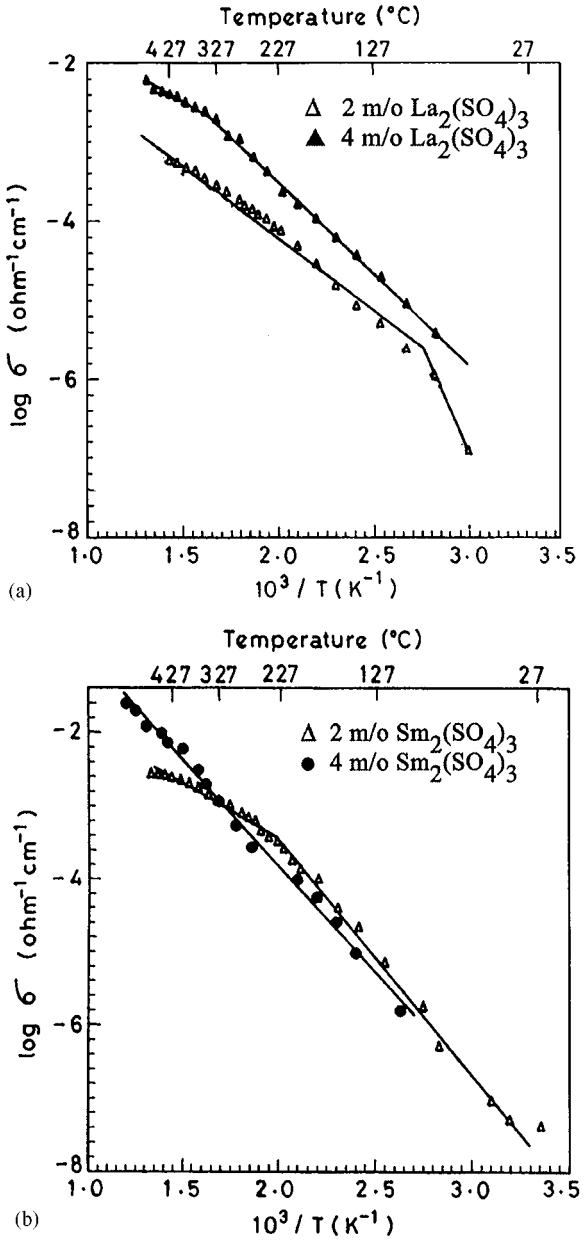

FIG. 2. (a) Log σ vs 10^3/T plots for the 2 and 4 m/o $La_2(SO_4)_3$-doped Na_2SO_4 compositions. (b) Log σ vs 10^3/T plots for the 2 and 4 m/o $Sm_2(SO_4)_3$-doped Na_2SO_4 compositions.

In Fig. 3, the plots of log σ vs 10^3/T for the 2 and 6 m/o $BaSO_4$ and $SrSO_4$ doped have been shown for comparison. This has been done to highlight the role of the size of the cation. Since these compositions are well below the solid solubility of the cations involved, which are certainly in excess of 17 m/o for both (39, 41), each Ba or Sr ion yields one Na^+ vacancy. Thus, if the hypothesis of Hofer *et al.* (33) were true, the conductivity for the 6 m/o Ba^{2+} and Sr^{2+} doped compositions, being dependent only on the amount of vacancy concentration should, within experimental error, be the same. We observe that the conductivity of the Sr^{2+}-doped compositions is higher than those of the corresponding Ba^{2+}-doped compositions. Thus, it appears that the size or some factor other than the vacancy concentration does indeed play a role and is discussed later. The maximum conductivity among the binary systems studied by Singhvi *et al.* (48) was reported for the 4 m/o Sm^{3+} and La^{3+} compositions, in agreement with the findings of Prakash and Shahi (35).

The importance of the contribution of Singhvi *et al.* (48) was that it established unequivocally the role of ionic size of the dopant on the conductivity of Na_2SO_4. Thus, two contradicting views (33, 35, 42) on whether the vacancy concentration alone influences the conductivity were resolved. In doing so, Singhvi *et al.* followed the scheme proposed by Hofer *et al.* (33) for calculating the vacancy concentrations. To nullify the effect of charge of the dopant cations, they plotted the dependence of conductivity on size for a fixed vacancy (6%) concentration, thus enabling the examination of the effect of size alone. The results of this exercise are presented in Fig. 4. Interestingly, a strong dependence of σ on the size of dopant is observed, and for a fixed 6 m/o vacancy concentration, the trend is clear. The data and a fit clearly show that the conductivity exhibits a maximum when the dopant size is comparable to that of Na^+.

Since the defects already exist in the form of vacancies due to the doping, the activation energy for the Na_2SO_4–I region, extracted from the conductivity plots, is the energy

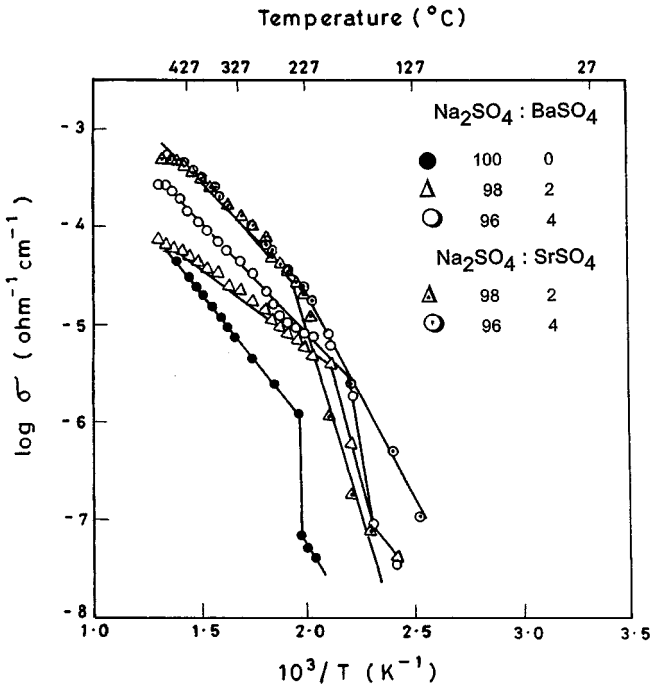

FIG. 3. Log σ vs 10^3/T plots for the x m/o $BaSO_4$ and $SrSO_4$-doped Na_2SO_4 compositions.

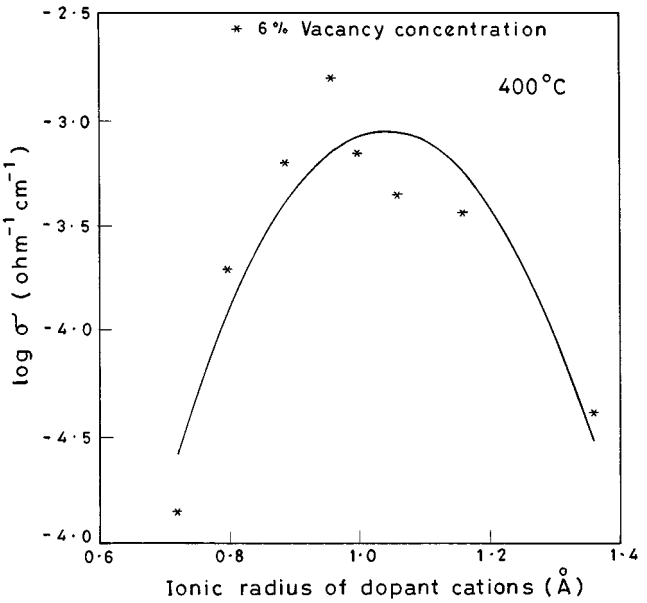

FIG. 4. Log σ vs ionic radii of the dopant cations at 400°C for 6% vacancy concentration.

associated with the migration of the Na^+ vacancies. From the work of Singhvi *et al.* (48), we have inferred that the activation energy of migration as a function of the ionic radii of the dopant exhibits an exactly inverted behavior to that shown for the log σ vs ionic size in Fig. 4. Obviously, this has been attributed to the ease of migration of Na^+ when the dopant has a size similar to that of the host cation, namely, Na^+. A smaller size dopant contracts the lattice, thereby increasing the energy of migration. A similar increase in the activation energy of migration for large-sized cations occurs due to the steric hindrance.

The ease of the solid solution formation with La^{3+} and Y^{3+} is reflected in the stabilization of the high-temperature phase at room temperature, observed from the peaks in our XRD, as well as the absence of the transition related peaks in the DSC results. In the case of La^{3+} and Sm^{3+}, with sizes comparable to Na^+, it appears that, upon cooling, the precipitation of the low-temperature phase becomes more difficult. Similar results on the stabilization of the cubic phase of ZrO_2 have been known to occur when the size of the host and the guest are almost the same (63, 64). The trivalent cations showed an enhancement dependence on size that is consistent with the earlier works of Prakash and Shahi (35).

In the present work, we have tried to address the issue of whether the conductivity measurements have been performed on samples containing a single phase. Also, this would help interpret the origin of the peaks in the DSC at or about 200°C reported by Singhvi *et al.* (48) for the various doped Na_2SO_4 compositions.

B. Homovalent Cation and Anion Substitution in Na_2SO_4

Anion substitutions have also had an equally important place in the development of this material as issues relating to the mechanism of conduction, discussed earlier, were resolved using a large number of homovalent impurities. Secco and coworkers (1, 3–6) were largely responsible for proposing the percolation model of conduction in Na_2SO_4. It was their investigations that conclusively proved that the anion-rotation cogwheel mechanism did not contribute to the conductivity of Na_2SO_4. In the absence of cation vacancies that arise only when aliovalent cations are used, Secco and coworkers argued that simple lattice expansion facilitates ionic mobility when other anions substitute for the SO_4^{2-} in the lattice. The studies of Leblanc *et al.* (5) on the conductivity for solid solutions of Na_2SO_4, K_2WO_4, Na_2MoO_4, Rb_2SO_4, Na_4SiO_4, and $Gd_2(SO_4)_3$ indicated in all cases, except K_2SO_4, an increase in Na^+ conductivity. Kumari *et al.* (6) predicted an increase in the conductivity of Na_2SO_4–I solid solution with Ag_2SO_4 owing to the isomorphism exhibited by both the low-temperature and high-temperature forms of Ag_2SO_4 and Na_2SO_4. The conductivity of the 40 m/o Ag_2SO_4-doped sample was found to be higher than that of Na_2SO_4 but lower than that of Ag_2SO_4. This was again attributed to the lattice expansion of Na_2SO_4 in the presence of Ag^+ ions and lattice contraction of the Ag_2SO_4 due to the Na^+ ions. Doping 4 m/o $CdSO_4$ in this binary composition increased the conductivity by almost an order of magnitude.

Studies on the Na_2SO_4–Na_3PO_4 system (65, 66) and Na_2SO_4–Na_2SeO_4 system (49) also showed an enhancement in conductivity of Na_2SO_4–I phase but did not stabilize that phase at lower temperatures. Prakash and Shahi investigated the Na_2SO_4–Na_2WO_4 system (35) and reported the presence of two conductivity maxima.

Chaklanobis *et al.* (50) investigated the Na_2SO_4–Li_2SO_4 system and reported the presence of two conductivity maxima occurring at $\sim$75 m/o Li_2SO_4 and 10 m/o Li_2SO_4 in the Na_2SO_4–Li_2SO_4 system. The enhancement in conductivity was observed to be just twice that of Na_2SO_4 in the former composition and $\sim$30 times at 300°C in the latter composition. This enhancement in conductivity was attributed to effects associated with the dispersion of fine particles of a second phase ($LiNaSO_4$).

Recently, Gomathy *et al.* (59) conducted a systematic investigation of the effect of homovalent anion doping on the conductivity and phase transitions in Na_2SO_4. They concluded that apart from the size, the shape, and the orientational ordering of the dopant ion in the sulfate sublattice appeared to influence the activation energy. It was also reported that the structure of the guest anion appeared to be the main factor determining the phase stabilization of Na_2SO_4–I at lower temperatures.

For the Na_2SO_4–Na_2CO_3 system (59), the 2 and 4 m/o compositions showed a smaller activation energy (45 and 40 kJ/mol), and also stabilized the Na_2SO_4–I phase. Gomathy *et al.* attribute this to the shape and orientation of the CO_3^{2-} in the sulfate lattice. According to Mehrotra *et al.* (55), the planar carbonate groups are oriented perpendicular to the *c*-axis in Na_2SO_4–I. Since the *c*/*a* ratio in pure and Na_2CO_3 doped Na_2SO_4 do not differ, it implies that there is no change in the bottleneck size for the diffusing Na^+ along directions in the *a*–*b* plane. However, Gomathy *et al.* (59) also observed that the orientational ordering is possible only to a limited extent, as phase I is stabilized only by the 2 and 4 m/o Na_2CO_3 compositions. At higher concentrations, it has been reported that the lattice contraction due to the smaller sized CO_3^{2-} becomes predominant, and increases the activation energy, resulting in a lower conductivity for the 5 m/o and the 10 m/o Na_2CO_3 compositions.

The conductivity results are summarized in Fig. 5. It can also be observed in Fig. 5 that the 5 m/o Na_2WO_4 composition exhibits a higher conductivity compared to the 5 m/o Na_2CO_3 composition. The lower activation energy for the Na_2WO_4-doped sample (40.8 kJ/mol for tungstate and 56.7 kJ/mol for carbonate) explains the behavior. The large WO_4^{2-} opens up the lattice, resulting in an ease of migration. On the other hand, a contracted lattice due to CO_3^{2-} doping makes it difficult for the Na^+ to diffuse.

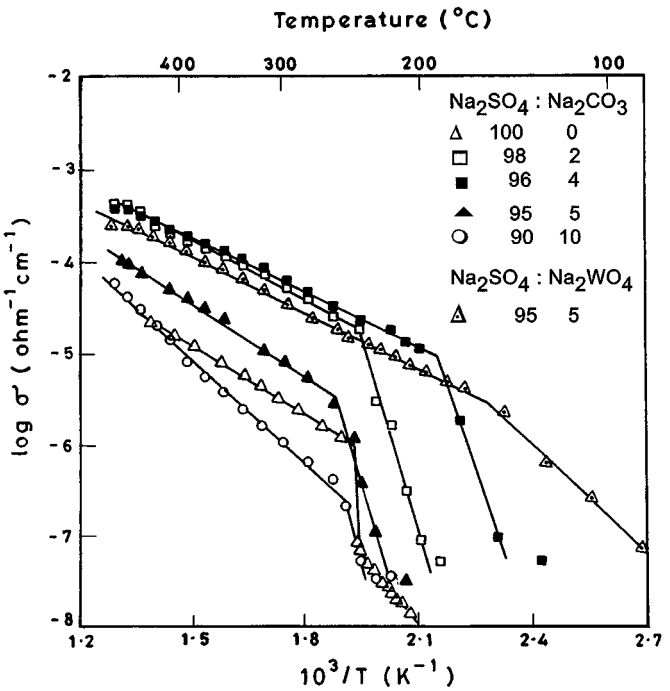

FIG. 5. Log σ vs 10^3/T for various compositions in the Na_2SO_4–Na_2CO_3 system. Note that the 5 m/o Na_2WO_4 composition has also been included for comparison.

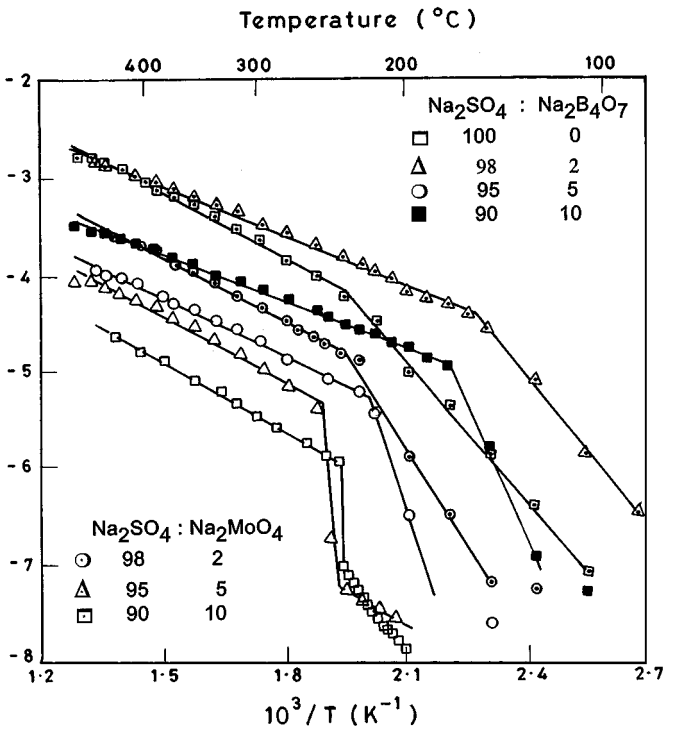

FIG. 6. Log σ vs 10^3/T for various compositions in the Na_2SO_4–$Na_2B_4O_7$ and Na_2SO_4–Na_2MoO_4 systems.

Figure 6 exhibits the conductivity *vs* temperature behavior for the $Na_2B_4O_7$ and Na_2MoO_4 compositions. For all the compositions, Gomathy *et al.* explained that the molybdate doped compositions have a higher conductivity due to a number of reasons. First, the larger size of the MoO_4^{2-} creates more free volume for ion migration. Second, the size mismatch between the molybdate and sulfate anions results in an increase of mobile Na ions. Third, the heavier MoO_4 ions impart stability to the anion sublattice, thereby reducing the scattering of the mobile Na ions. Last, the high-temperature forms of Na_2SO_4 and Na_2MoO_4 are isomorphous, resulting in a higher solid solubility of the MoO_4 ions in the sulfate lattice.

As for the $B_4O_7^{2-}$ compositions, the activation energies are higher compared to the corresponding MoO_4^{2-} compositions. Only the 10 m/o $B_4O_7^{2-}$ composition is an exception. The formation of a glassy phase may possibly explain the lower activation energy.

C. *Na_2SO_4-Based Composites*

The ionic conductivity of several solid electrolytes has been increased significantly, from one to three orders of magnitude, by dispersing fine submicrometer, insulating particles of a second phase (67–70). The mechanisms for conductivity enhancement in composites, however, still

remain ambiguous. It is widely accepted that unlike homogeneous doping, local deviation from electroneutrality plays an important role in heterogeneous doping (71). Various mechanisms involving both the matrix and the matrix-dispersoid interface have been reported in literature to explain the *composite effect* (72–74).

The *interface mechanisms* (72) are likely to arise from one or a combination of the three factors; a space-charge layer formation at the matrix–particle interface, enhanced conduction at the core of the interface, and interfacial phase formation and effects of adsorbed surface moisture and impurities.

Likewise, the *matrix mechanisms* (73) are likely to have a contribution from one or a combination of the following: an enhanced charge transportation along grain – boundaries and dislocations, stabilization of highly conducting metastable phases due to the dispersoid, and homogeneous doping of the matrix. In general, no chemical reaction is found to occur between the matrix and the dispersoid. Maier has contributed significantly to explain the origin of conductivity enhancement in composite electrolyte systems (75–81).

Of the nearly 20 composite systems researched to date, the most well studied system is LiI, where the conductivity increases by three orders of magnitude when dispersed with 40 m/o Al_2O_3 (67).

As for sulfates, only two reports exist in the literature. It was shown that the ionic conductivity of the low temperature phase of Li_2SO_4 increases by three orders of magnitude when dispersed with 47 m/o Al_2O_3 (82). Very recently, Jain *et al.* (60) have reported results on the Na_2SO_4–Al_2O_3 system. Through a systematic investigation involving compositions between 1 and 50 m/o Al_2O_3, Jain *et al.* concluded that the largest enhancement in conductivity for furnace cooled samples is observed for 5.5 and 35 m/o Al_2O_3 compositions. For the 35 m/o composition, the conductivity increases by more than one order of magnitude at 400°C, and two orders of magnitude at 200°C. Figures 7 and 8 exhibit the log (σT) vs 10^3/T plots for the various Na_2SO_4–Al_2O_3 compositions, the exception being the 5 m/o Al_2O_3 composition in Fig. 7, which has been investigated as part of the present work. A discussion of the observations, therefore, follows in a later section.

In contrast to an understanding based on many composite electrolyte theories, Jain *et al.* (60) reported that 0.004-μm alumina brings about the same or even a lower enhancement in conductivity as 0.5-μm alumina. Furthermore, contrary to expectations, negligible enhancement was observed by employing γ-Al_2O_3. The enhancements in the conductivity for Na_2SO_4 have been observed only when the identified phase is α-Al_2O_3.

Unlike in any other known composite system, Jain *et al.* reported the presence of two maxima in the conductivity vs composition for the Na_2SO_4–Al_2O_3 system. They attributed the maximum observed at 5.5 m/o Al_2O_3 to a percolation mechanism (83) and that at 35 m/o Al_2O_3 to dispersoid-induced changes in the bulk (84). Moreover, they also modeled the results for this system and concluded that a combination of mechanisms alone can explain the observations. The conductivity behavior of the Na_2SO_4–Al_2O_3 system turned out to be a combination of the Type II and Type III behaviors suggested by Brailsford (85).

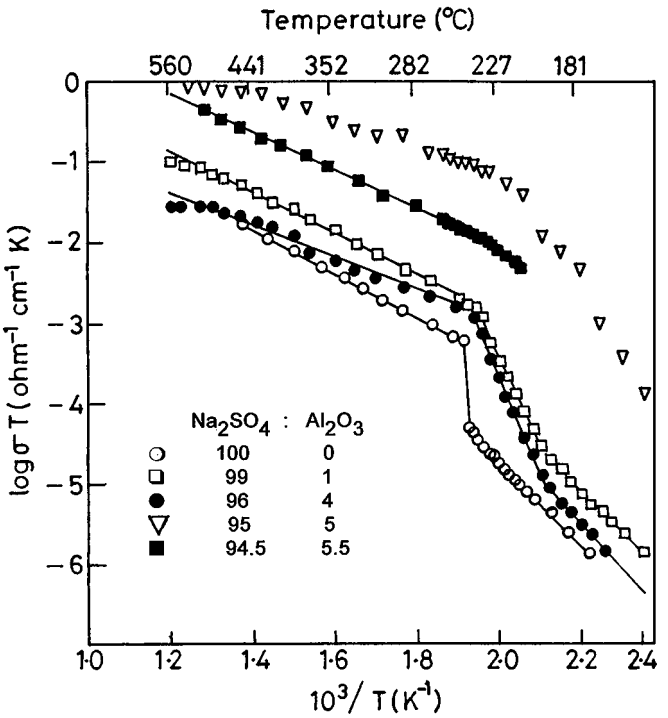

FIG. 7. Log σT vs 10^3/T for x m/o ($x < 10$) α-Al_2O_3 (0.5 μm) compositions.

The Type II behavior is characterized by a smooth maximum and is attributed to dispersoid-induced changes in the bulk conductivity, accounting for the maxima observed for the 35 m/o Al_2O_3 composition. The Type III behavior on the other hand, identified by a sharp and abrupt maximum, attributed primarily to locally enhanced conduction around the dispersoid; i.e., the interface mechanism is dominant in this regime (85). In the case of the Na_2SO_4–Al_2O_3 system, Jain *et al.* (60) argued that the Type III behavior is reflected by the 5.5 m/o Al_2O_3 composition. Last, while examining the role of a few preparatory parameters, Jain *et al.* proposed that a reduction in the grain size of the matrix, and a quenching of the samples, rather than furnace cooling, might result in further enhancement in the conductivity.

The maximum enhancement in the conductivity reported by Jain *et al.* was for the 4 m/o Al_2O_3 quenched sample. The conductivity increased by two orders for the high-temperature phase and by more than three orders for the low-temperature phase of Na_2SO_4.

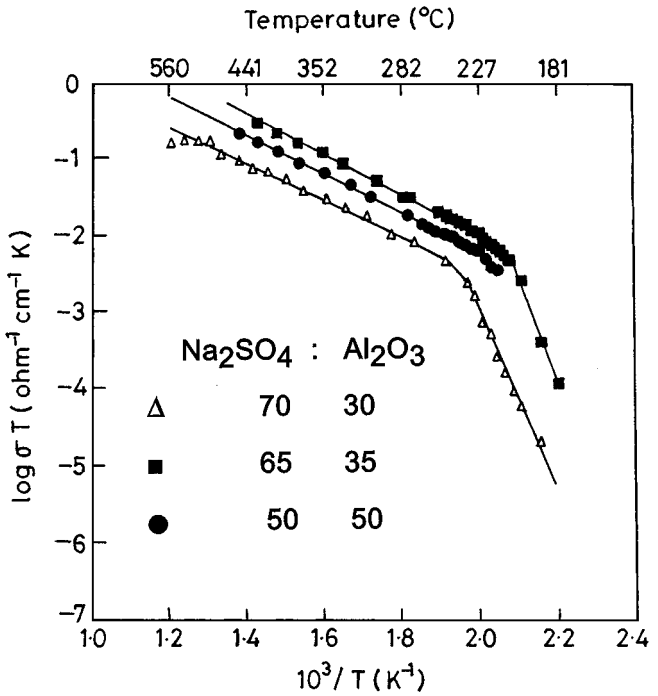

FIG. 8. Log σT vs $10^3/T$ for x m/o ($x > 10$) α-Al_2O_3 (0.5 μm) compositions.

It appears from the existing literature that certain questions need to be addressed immediately. The binary sulfate systems invariably show peaks in the DSC at temperatures between 200 and 250°C. Do these always correspond to phase transitions in Na_2SO_4? This is particularly important in the case of binary systems where the conductivity–temperature behavior appears to indicate a stabilization of the high-conducting, high-temperature Na_2SO_4–I at temperatures much below those corresponding to the DSC peaks. Only a high-temperature XRD study can help answer the questions. This work addresses the issue of the relationship between transitions observed in the $\sigma(T)$ behavior and those observed in DSC.

Further, it is not easy to believe that the 5.5 m/o Al_2O_3 composition results in a large enhancement in conductivity due to the opening of percolation pathways. Last, a number of newer aspects, relating to the role of preparatory parameters on the properties of the Na_2SO_4–Al_2O_3 system need to be investigated. In this work, we have attempted to reduce the grain size of Na_2SO_4 through a spray drying technique, quenched the composites, and also investigated additional compositions around 5.5 and 35 m/o Al_2O_3 that had previously exhibited the maximum conductivity.

3. EXPERIMENTAL WORK

For sample preparation, all sulfates of purity in excess of 99.9% were procured from Aldrich Chemicals. Three compositions were prepared for the high-temperature XRD work. A composition containing 6 m/o of the dopant concentration for the Na_2SO_4–$ZnSO_4$, one containing 4 m/o $Sm_2(SO_4)_3$ composition in the Na_2SO_4–$Sm_2(SO_4)_3$, and the last containing 4 m/o $La_2(SO_4)_3$ in the Na_2SO_4–$La_2(SO_4)_3$ system, were prepared by melting the charge and quenching on brass moulds in air. The high-temperature XRD experiments were performed on a Siemens D5000 diffractometer, using Cu$K\alpha$ radiation and a hot stage developed in-house, at several temperatures between 25 and 300°C.

For the composite formation, Al_2O_3 was prepared from a sol using Disperal Sol P3 procured from Condea Chemie (Germany). In addition, finely sized Al_2O_3 of particle size ~40 Å was prepared by reacting ultraclean pieces of Al with 0.1 N mercuric chloride and subsequently dissolving in water and making the particles settle in a solution of 2-ethyl hexanol and Span 80, followed by drying under infrared radiation. The particles were characterized using surface area measurement techniques and TEM.

To study the effect of preparation techniques on the conductivity, the composites were prepared by the chemical as well as the spray-drying route. Sodium sulfate and alumina were mixed in appropriate mole percentages and stirred thoroughly in deionized water. The slurry was then slowly heated in an oven to facilitate the evaporation of water. The mixtures were then heated for 24 h to a temperature of 1000°C to facilitate a fine dispersal of α-Al_2O_3 or 600°C for γ-Al_2O_3. The samples were then furnace cooled, ground to a fine powder, and pelletized at pressures of approximately 5 tons/cm^2. The resulting pellets were 2–4 mm thick and around 12 mm in diameter. In addition, a second set of samples for certain compositions were prepared by quenching them in air after an identical heat treatment to provide the basis for a comparative study. These pellets were then sintered at 600°C for 8 h and gold-coated to ensure good electrical contact with the Pt electrodes during impedance measurements. Subsequently, a wide range of compositions varying from 0 to 50 m/o Al_2O_3 were prepared in this study.

To allow better dispersion of the Al_2O_3 particles and produce a finer sized precursor powder, two of the compositions (namely, 5 and 33 m/o Al_2O_3) were also prepared using the spray drying technique. To prevent any precipitation in the sol and thereby avoid segregation of alumina in the composite, Triton X-100 was added as a surfactant.

4. RESULTS AND DISCUSSION

A. High-Temperature XRD for Cation Substitution in Na_2SO_4

The XRD for the 4 m/o Na_2SO_4–$La_2(SO_4)_3$ composition carried out at 120°C, chosen as the representative composition, has been exhibited in Fig. 9. It can be observed that most of the lines in the pattern can be indexed to the

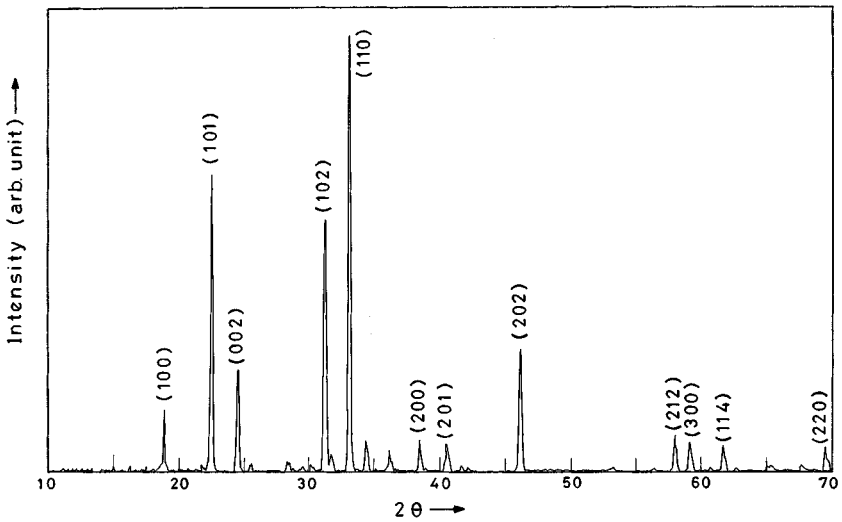

FIG. 9. XRD pattern at 120°C for a 4 m/o $La_2(SO_4)_3$-doped Na_2SO_4 composition.

high-temperature Na_2SO_4–I. Thus, the stabilization of this phase at 120°C is now established through structural evidence. This has been lacking in all earlier works and the slopes of the conductivity–temperature plots were often brought into discussion to justify an existence of Na_2SO_4–I. As a result of the high-temperature XRD experiments, the peaks in the DSC observed at 255 and 275°C can now be correlated to events other than the phase transitions in Na_2SO_4. Furthermore, another question uppermost in many minds has been the phase purity, namely, if the compositions are single or multiphase. The XRD in Fig. 9 clearly indicates that we are dealing with a single-phase sample, barring two small peaks that appear insignificant and could not be associated with any known phase in the binary. Our XRD results show that the two peaks eventually disappear at temperatures around 220°C. In interpreting the conductivity results for doped Na_2SO_4 compositions, the large solid-solubility of the high-temperature phase has been extensively quoted, and little done to substantiate any claims. These results now provide a clear evidence for much of what was taken for granted in Na_2SO_4-based systems.

B. Na_2SO_4–Al_2O_3 Composites

Figure 7 exhibits the log σT *vs* 10^3/T for the 0, 1, 4, 5, and 5.5 m/o α-Al_2O_3 composition, whereas the 30, 35, and 50 m/o α-Al_2O_3 compositions are depicted in Fig. 8. For the Na_2SO_4 (I) phase (in the temperature range T_c–550°C), the plots are indicative of a classical Arrhenius type dependence. In this work, a distinct trend has been observed for variation of the activation energy with alumina composition in this temperature range (see Table 3).

For the 5 m/o Al_2O_3 composition, the conductivity increased by a factor of 60 at 400°C ($\sigma = 8.3 \times 10^{-4}$ S/cm) and almost 2000 times at 200°C ($\sigma = 2.5 \times 10^{-5}$ S/cm). This enhancement is almost comparable with that of the prototype Li_2SO_4–Al_2O_3 system where an enhancement of about 3 orders of magnitude is achieved around the 48 m/o composition (82). For the 35 m/o Al_2O_3 composition, an enhancement by a factor of 23 at 400°C ($\sigma = 3.16 \times 10^{-4}$ S/cm) and 450 times at 200°C ($\sigma = 5.6 \times 10^{-6}$ S/cm) could be achieved. The relevant data for some of the compositions studied during the course of this work has been presented in Table 3.

An interesting feature presented in Table 3 is the variation in activation energy with composition. One observes

TABLE 3
Relevant Data for Electrical Characteristics of Na_2SO_4–Al_2O_3 Composites

Composition (m/o Al_2O_3)	σ/σ_{pure}		E_a (eV) (T_c − 550°C)
	At 200°C	At 400°C	
0	1	1	0.49
1	5	3	0.50
5	2016	63	0.21–0.25
5.5	263	17	0.47
10	45	8	0.46
20	91	8	0.56
30	10	6	0.47
33	290	9	0.35
35	457	23	0.52
40	275	18	0.45

Note. σ_{pure} refers to the conductivity of pure Na_2SO_4.

a sharp drop in the activation energy near the 5 m/o Al_2O_3 composition, corresponding to the abrupt enhancement in conductivity. This feature appears to be in agreement with the model proposed by Roman *et al.* (83), wherein an enhancement in conductivity is accompanied by a corresponding fall in the activation energy. Although the same feature is not so evident in the higher alumina composition range, one does observe a lowering of E_a around the 33 m/o composition, which marks the onset of the second maxima. These observations are suggestive of the fact that perhaps different conductivity enhancement mechanisms are dominant in the two different composition regimes. The low E_a value in the low alumina composition region probably reflects only the activation energy for the migration of defects, whereas the higher values around the 35 m/o alumina composition point toward the generation of defects in the bulk of the matrix. Dudney (72), in a review of the "composite effect" had pointed out that the enhancement of conductivity in composites could be the consequence of multiple mechanisms operating simultaneously. This conjecture is perhaps best vindicated by the results obtained for the Na_2SO_4–Al_2O_3 system.

As pointed out by Jain *et al.* (60), experimental data do seem to suggest that the sharp peak around the 5 m/o alumina composition is a consequence of the percolation mechanism propounded by Roman *et al.* (86). However, it appears that 5 m/o Al_2O_3 is unlikely to meet the requirement for the formation of a percolation network. Usually the percolation threshold would require a volume fraction of 25% or more of Al_2O_3, depending on the particle size of the two phases. On the other hand, the peak at the 35 m/o composition appears to be a characteristic of the bulk mechanism. Our modeling endeavors, although successful only to a limited extent, appear to accommodate these inferences reasonably satisfactorily. The conductivity behavior of the Na_2SO_4– Al_2O_3 system turns out to be a combination of the Type II and Type III behavior suggested by Brailsford (85). As stated before, the Type II behavior is characterized by a smooth maximum and is attributed to dispersoid induced changes in the bulk conductivity. On the other hand, the Type III behavior can be identified by a sharp and abrupt maximum arising due to locally enhanced conduction around the dispersoid.

However, a startling aspect, not observed in the work of Jain *et al.* (60), emerged in the present investigations. The XRD results presented perhaps the most intriguing feature of our studies. Although no reaction was generally found to occur between the matrix and the dispersoid corroborating the results for most other systems, there was, however, one major exception. For the 5 m/o alumina composite, in addition to Na_2SO_4–V (dominant phase), there were peaks corresponding to an intermediate high-conducting phase, Na β-alumina. The XRD for the 5 m/o composition is shown in Fig. 10. All the other compositions exhibited peaks for only Na_2SO_4 (phases V, III) and/or alumina (α, γ), in agreement with the observations of Jain *et al.* (60).

It is very difficult to interpret the apparent absence of Na β-alumina when the composition changes even slightly. Perhaps this explains why Jain *et al.* (60) missed the Na β-alumina phase, as the 5 m/o Al_2O_3 was not investigated in their work. However, with compositions such as 4 and 5.5 m/o Al_2O_3 that were investigated, they could not see any signature of the Na β-alumina phase, in agreement with our observations.

The low activation energy and the maximum enhancement for the 5 m/o alumina composition also reflect the presence of Na β-alumina, which is a recognized superionic conductor. It is also to be noted here that the peaks for Na

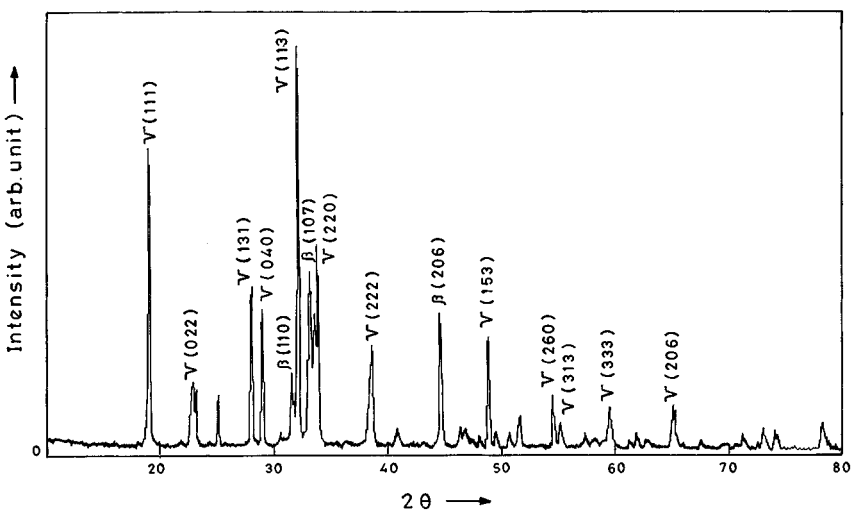

FIG. 10. XRD pattern for a 5 m/o Al_2O_3-doped composition. Note that the only two phases present are Na_2SO_4–V and Na β-alumina.

β-alumina, which was absent in all the other compositions, were again found to be present in the 5 m/o composition prepared differently by the spray drying route, thereby confirming the reproducibility of the experiments. It is worth mentioning here that in the prototype Li_2SO_4–Al_2O_3 system, an intermediate phase, γ-$LiAlO_2$, was reported to form. The occurrence of this phase actually lowered the conductivity of the system (87).

Most theories on composite electrolyte state an inverse relationship between the conductivity and particle size of the dispersoid. Accordingly, alumina of particle size varying from 0.5 μm to 40 Å was used to prepare the composites but no further enhancement in conductivity could be effected, in agreement with earlier findings (60). The fact that for the 35 m/o composition, 0.5-μm alumina produced greater enhancement than 40-Å alumina is itself a deviation from known theories. However, whether the final grain size of alumina was still submicrometer after heat treatment is debatable. In fact, SEM studies tended to indicate that there was indeed some grain growth and agglomeration of the fine-grained dispersoid, which would probably explain the observed behavior.

To delve further into the role of preparatory conditions, the 5 and 33 m/o alumina composites were prepared by spray drying. This was carried out to reduce the matrix grain size, which also is believed to play a role in conductivity enhancement (72, 74). However, no further improvement in the conductivity could be effected, although the resultant powder was of appreciably finer particle size. The particle size analysis of the resultant powder indicated the average grain size to be approximately 8 μm, indicating an agglomeration of very fine particles of powder. The agglomeration of very fine powders and grain growth after heat treatment has been presumably detrimental to the composite effect.

Another technique was applied to determine the role of grain size in the conductivity enhancement process. Some of the compositions were prepared by quenching them in air after heat treatment, while identical compositions were also prepared by furnace cooling. Since the grain size is sensitive to preparatory parameters, the quenched and furnace-cooled samples were expected to provide a base for comparative study. The log σ vs 1000/T plots for the 4 and 6 m/o alumina composites are shown in Fig. 11. While there was no difference between the furnace-cooled and quenched composites for the higher alumina compositions, the quenched samples for the lower alumina composites showed a definite enhancement in conductivity, except for the 5 m/o alumina composition. The conductivity of the 4 m/o quenched sample exhibited an enhancement by a factor of 30 at 400°C ($\sigma = 3.94 \times 10^{-4}$ S/cm) and 3129 times at 200°C ($\sigma = 3.88 \times 10^{-5}$ S/cm) compared to pure Na_2SO_4. This is clearly comparable to the enhancement observed for the 5 m/o alumina composition, where the dominant contribution comes from the highly conducting β-alumina. However,

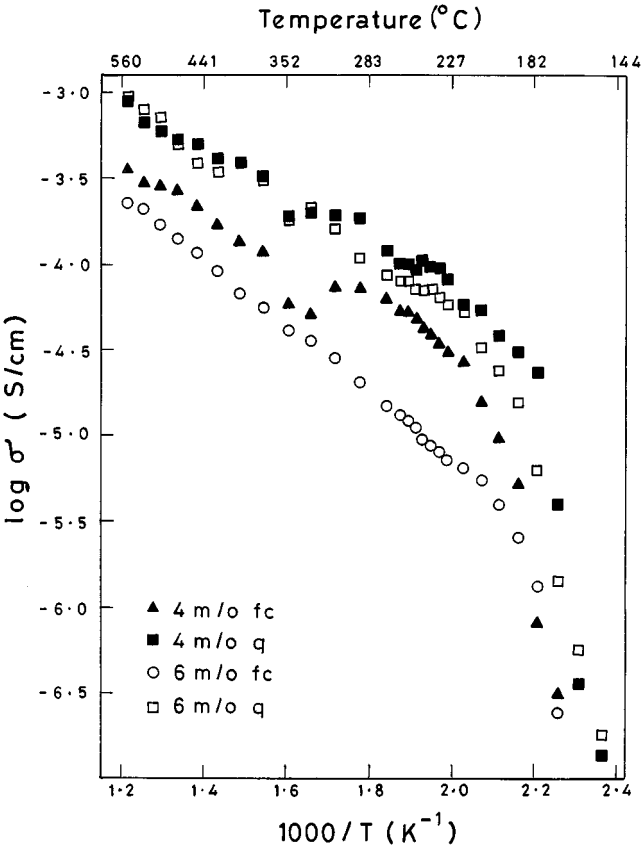

FIG. 11. Log σT vs 10^3/T for 4 and 6 m/o α-Al_2O_3, both furnace-cooled as well as quenched compositions.

at this time, we have been unable to detect the presence of the high conducting Na β-alumina in the XRD for the 4 m/o composition. Finally, SEM studies have shown that there is an overall uniform dispersion of alumina for the 35 m/o alumina composition but for the 5 m/o alumina composite, the dispersed alumina appears to be highly agglomerated forming isolated clusters. This again is contradictory to the requirements for setting up a percolation network throughout the sample. This is, therefore, again synonymous with the interface mechanism for the lower alumina compositions.

5. CONCLUSIONS

It is evident that a large body of work on the electrical properties of Na_2SO_4 has accumulated in the literature. Cation doping, anion doping, and the composite electrolyte formation have been the three strategies adopted for obtaining large conductivity enhancements. The mechanism of conduction is known and clearly understood in this material. It appears that an enhancement of over three orders of magnitude was also possible in both the low- and the high-temperature phases of Na_2SO_4.

It appears that the usual methods of enhancing conductivity are not likely to result in any substantial improvement over and above what is already known. However, serious issues like the defect structure of Na_2SO_4 have still not been addressed comprehensively and need to be examined. Only a detailed idea of the defect structure may open up fresh avenues for enhancing the conductivity using the traditional approaches.

The high-temperature XRD results have clearly established the stabilization of the high-temperature Na_2SO_4–I at about 100°C. The origin of the peaks in DSC above 100°C has now been resolved as originating from transitions other than those associated with Na_2SO_4.

Interestingly, there have been some developments on Na_2SO_4-based composite electrolytes. In the few investigations that they have attracted, a number of interesting observations have come up. To date, all known composite electrolytes have displayed only a single peak in the conductivity–composition behavior. Furthermore, the enhancements have mostly been observed in almost all systems when γ-Al_2O_3 was used. In both these respects, the Na_2SO_4–Al_2O_3 composites have behaved differently. While two peaks, one at 5 m/o and the other at 35 m/o Al_2O_3, have been observed in the conductivity–composition plots, the enhancements have also been observed only when α-alumina was used. Little or no enhancement was observed for γ-Al_2O_3.

While it is well known for composites that the conductivity enhancements are large when the dispersoid size is small, the observations in the Na_2SO_4–Al_2O_3 indicate that 0.004- and 0.5-μm alumina bring about the same increase. In some compositions, the 0.004-μm alumina has actually resulted in a lower conductivity. This issue needs to be explored further. Last, there are not many illustrations in the composite electrolyte literature where intermediate phases have formed, resulting in conductivity enhancements. In the Na_2SO_4–Al_2O_3 system, our XRD results clearly exhibit the existence of the high-conducting Na β-alumina phase, albeit over a narrow composition range. This again raises interesting possibility of investigating and optimizing the conditions under which the high-conducting Na β-alumina phase may be favorably formed, particularly since all the processing is carried out at temperatures below 1000°C. We are presently concentrating our efforts in this direction.

In conclusion, it might be said that the Na_2SO_4–Al_2O_3 system, though presenting a number of features contradictory to accepted theories on composite electrolytes, did appear to follow a particular trend. It appears that the interface, and not the percolation mechanism dominates for the lower alumina compositions, whereas the matrix mechanism is dominant in the higher alumina regimes. The formation of the highly conducting β-alumina further contributes to the conductivity process and raises interesting questions in this particular system. The system also offers interesting possibilities for theoretical modeling of the observed conductivity behavior.

ACKNOWLEDGMENTS

This paper is dedicated to Professor J. M. Honig, who has retired after an illustrious and distinguished career at Purdue University. One of us (P.G.), who obtained a doctorate under the supervision of Professors J. M. Honig and J. Spałek, wishes to express his gratitude and respect to a great teacher and a thesis advisor, for having provided invaluable guidance, in and out of the laboratory, at all times of need. His work ethic and dedication to the area of solid state chemistry will always continue to be a source for inspiration. His friendship will always be remembered fondly. The authors express their sincere thanks to Mr. S. L. Kamath for performing the DSC experiments. One of the authors (S.B.) was supported by a research funding from DRDO, Government of India.

REFERENCES

1. E. A. Secco, *in* "Solid State Ionics—Materials and Applications" (B. V. R. Chowdari, S. Singh, S. Chandra, and P. C. Srivastava, Eds.), p. 47. World Scientific, Singapore, 1992.
2. A. Kvist and A. Bengtzelius, *in* "Fast Ion Transport in Solids" (W. Van Gool, Ed.), 193. North-Holland, Amsterdam, 1973.
3. E. A. Secco, *Phys. Status Solidi* (*a*) **88,** K75 (1985).
4. R. A. Secco and E. A. Secco, *J. Phys. Chem. Solids* **53,** 749 (1992).
5. M. D. Leblanc, U. M. Gundusharma, and E. A. Secco, *Solid State Ionics* **20,** 61 (1986).
6. M. S. Kumari and E. A. Secco, *Can. J. Chem.* **61,** 2804 (1983).
7. A. Lunden, *Solid State Ionics* **76,** 249 (1995).
8. A. Lunden and M. A. K. L. Dissanayake, *J. Solid State Chem.* **90,** 179 (1991).
9. N. H. Anderson, P. W. S. K. Bandaranayake, M. A. Careem, M. A. K. L. Dissanayake, C. N. Wijayasekera, R. Kaber, A. Lunden, B.-E. Mellander, L. Nilsson, and J. O. Thomas, *Solid State Ionics* **57,** 203 (1992).
10. A. Lunden, *Solid State Ionics* **28–30,** 163 (1988).
11. E. A. Secco, *Solid State Ionics* **60,** 233 (1993).
12. E. A. Secco, *J. Solid State Chem.* **96,** 366 (1992).
13. A. S. Campbell, K. G. MacDonald, and E. A. Secco, *J. Solid State Chem.* **81,** 65 (1989).
14. U. M. Gundusharma and E. A. Secco, *Appl. Phys. A* **51,** 7 (1990).
15. E. A. Secco, *Solid State Commun.* **66,** 921 (1988); U. M. Gundusharma, C. MacLean, and E. A. Secco, *Solid State Commun.* **57,** 479 (1986).
16. M. Jansen, *Angew. Chem. Int. Ed. Engl.* **30,** 1549 (1991).
17. L. Karlson and R. L. McGreevy, *Solid State Ionics* **76,** 301 (1995).
18. M. Gauthier and A. Chamberland, *J. Electrochem. Soc.* **124,** 1579 (1977).
19. M. Gauthier, R. Bellemare, and A. Belanger, *J. Electrochem. Soc.* **128,** 371 (1981).
20. N. Imanaka, Y. Yamaguchi, S. Kuwabara, G. Y. Adachi, and J. Shiokawa, *Bull. Chem. Soc. Jpn.* **58,** 5 (1985); *Solid State Ionics* **23,** 15 (1987).
21. T. Maruyama, Y. Saito, Y. Matsumoto, and Y. Yano, *Solid State Ionics* **17,** 281 (1985).
22. N. Imanaka, Y. Yamaguchi, S. Kuwabara, G. Y. Adachi, and J. Shiokawa, *Solid State Ionics* **20,** 153 (1986); *J. Electrochem. Soc.* **133,** 1026 (1986).
23. K. T. Jacob, M. Iwase, and Y. Waseda, *Solid State Ionics* **23,** 245 (1987).
24. R. Akila and K. T. Jacob, *J. Appl. Electrochem.* **18,** 245 (1988).
25. W. L. Worrell, *Chem. Sensor Technol.* **1,** 97 (1988).

26. G. Rog, A. Kozlowska-Rog, K. Zakula, W. Bogusz, and W. Pucior, *J. Appl. Electrochem.* **21,** 308 (1991).
27. Y. Yan, Y. Shimitzu, N. Miura, and N. Yamazoe, *Sensors Actuators B* **12,** 77 (1993).
28. Y. Yan, Y. Shimitzu, N. Miura, and N. Yamazoe, *Sensors Actuators B* **20,** 81 (1994).
29. A. Lunden, *Solid State Commun.* **65,** 1237 (1988).
30. L. Borjesson and L. M. Torell, *Phys. Rev. B* **32,** 2471 (1985).
31. R. M. Murray and E. A. Secco, *Can. J. Chem.* **56,** 2616 (1978).
32. K. L. Keester, W. Eysel, and Th. Hahn, *Acta Crystallogr. A* **31,** S79 (1975).
33. H. H. Hofer, W. Eysel, and U. Von Alpen, *Mater. Res. Bull.* **13,** 135 (1978); *J. Solid State Chem.* **36,** 365 (1981).
34. K. Shahi and G. Prakash, *Solid State Ionics* **18/19,** 544 (1986).
35. G. Prakash and K. Shahi, *Solid State Ionics* **23,** 151 (1987).
36. R. Frech and G. Dharmasena, *Solid State Ionics* **70/71,** 191 (1994).
37. G. Dharmasena and R. Frech, *J. Chem. Phys.* **99,** 8929 (1993).
38. N. Rao and J. Schoonman, *Solid State Ionics* **57,** 159 (1992).
39. Y. Saito, K. Kobayashi, and T. Maruyama, *Solid State Ionics* **3/4,** 687 (1981).
40. Y. Saito, K. Kobayashi, and T. Maruyama, *Solid State Ionics* **14,** 265 (1984).
41. W. Eysel, H. H. Hofer, K. L. Keester, and Th. Hahn, *Acta. Crystallogr. B* **41,** 5 (1985).
42. E. A. Secco and M. G. Usha, *Solid State Ionics* **68,** 213 (1994).
43. M. Ohta and M. Sakaguchi, *J. Solid State Chem.* **91,** 57 (1991).
44. S. Chaklanobis, R. K. Syal, and K. Shahi, *in* "Solid State Ionics—Materials and Applications" (B. V. R. Chowdari, S. Singh, S. Chandra, and P. C. Srivastava, Eds.), p. 441. World Scientific, Singapore, 1992.
45. P. W. S. K. Bandaranayake and B. E. Mellander, *Solid State Ionics* **40/41,** 31 (1990).
46. P. W. S. K. Bandaranayake and B. E. Mellander, *Solid State Ionics* **26,** 33 (1988).
47. N. Imanaka, G. Y. Adachi, and J. Shiokawa, *Bull. Chem. Soc. Jpn.* **57,** 687 (1984).
48. A. Singhvi, S. Gomathy, P. Gopalan, and A. R. Kulkarni, *J. Solid State Chem.* **138,** 183 (1998).
49. M. A. K. L. Dissanayake, M. A. Careem, P. W. S. K. Bandaranayake, R. Frech, and G. Dharmasena, *in* "Proceedings of the 2nd Asian Conference on Solid State Ionics—Beijing, Oct.–Nov. 1990" (B. V. R. Chowdari, Q. Liu, and L. Chen, Eds.), p. 435. World Scientific, Singapore.
50. S. Chaklanobis, K. Shahi, and R. K. Syal, *Solid State Ionics* **44,** 107 (1990).
51. A. N. Khlapova and E. S. Kovaleva, *J. Struct. Chem.* **67,** 517 (1963).
52. L. Chen, S. Yang, L. Zhao, M. Zhang, and D. Li, *in* "Proceedings of the 2nd Asian Conference on Solid State Ionics—Beijing, Oct.—Nov. 1990" (B. V. R. Chowdari, Q. Liu, and L. Chen, Eds.), p. 435. World Scientific, Singapore.
53. P. H. Bottleberghs and F. R. Van Buren, *J. Solid State Chem.* **13,** 182 (1975).
54. H. E. Boeke, *Z. Anorg. Chem.* **50,** 364 (1907).
55. B. N. Mehrotra, Th. Hahn, H. Arnold, and W. Eysel, *Acta Crystallogr. A* **31,** S79 (1975).
56. M. A. K. L. Dissanayake, M. A. Careem, P. W. S. K. Bandaranayake, R. P. Gunawardane, and C. N. Wijayasekera, *Solid State Ionics* **40/41,** 23 (1990).
57. M. A. K. L. Dissanayake and B. E. Mellander, *Solid State Ionics* **21,** 279 (1986).
58. M. A. Bredig, *J. Phys. Chem.* **46,** 247 (1942).
59. S. Gomathy, P. Gopalan, and A. R. Kulkarni, *J. Solid State Chem.* **146,** 6 (1999).
60. A. Jain, S. Saha, P. Gopalan, and A. Kulkarni, *J. Solid State Chem.*, in press.
61. F. C. Kracek and R. E. Gibson, *J. Phys. Chem.* **34,** 188 (1930).
62. R. D. Shannon and C. T. Prewitt, *Acta. Crystallogr. B* **25,** 925 (1969).
63. T. Kudo and H. Obayashi, *J. Electrochem. Soc.* **123,** 415 (1976).
64. F. H. Etsell and S. N. Flengas, *Chem. Rev.* **70,** 339 (1970).
65. H. Hruschka, E. Lissel, and M. Jansen, *Solid State Ionics* **28–30,** 159 (1988).
66. M. Dekker, R. A. Kalwij, J. Schram, and J. Schoonman, *Solid State Ionics* **28–30,** 1682 (1988).
67. C. C. Liang, *J. Electrochem. Soc.* **120,** 1289 (1973).
68. P. Chowdhary, V. B. Tare, and J. B. Wagner, Jr., *J. Electrochem. Soc.* **132,** 123 (1985).
69. J. B. Wagner, Jr., *Mater. Res. Bull.* **15,** 1691 (1980).
70. T. Jow and J. B. Wagner, Jr., *J. Electrochem. Soc.* **126,** 1973 (1979).
71. J. Maier, *in* "Heterogeneous Solid Electrolytes: Superionic Solids and Solid Electrolytes — Recent Trends" (A. Laskar and S. Chandra, Eds.), p. 137. Academic Press, New York, 1989.
72. N. J. Dudney, *Annu. Rev. Mater. Sci.* **19,** 103 (1989).
73. N. J. Dudney, *Solid State Ionics* **28–30,** 1065 (1988).
74. N. J. Dudney, *J. Am. Ceram. Soc.* **68,** 538 (1985).
75. J. Maier, *Phys. Stat. Sol.* (*b*) **123,** K89 (1984).
76. J. Maier, *Ber. Bunsenges. Phys. Chem.* **88,** 1057 (1984).
77. J. Maier, *J. Phys. Chem. Solids.* **46,** 309 (1985).
78. J. Maier, *J. Electrochem. Soc.* **134,** 1524 (1987).
79. J. Maier, *Prog. Solid State Chem.* **23,** 171 (1995).
80. J. Maier, *Solid State Ionics* **75,** 139 (1995).
81. J. Maier, *J. Eur. Ceram. Soc.* **19,** 675 (1999).
82. B. Zhu, Z. H. Lai, and B. E. Mellander, *Solid State Ionics* **70/71,** 125 (1994).
83. H. E. Roman, A. Bunde, and W. Dietrich, *Phys. Rev. B* **34,** 3479 (1986).
84. C. Wagner, *J. Phys. Chem. Solids* **33,** 1051 (1972).
85. A. D. Brailsford, *Solid State Ionics* **21,** 159 (1986).
86. E. Roman, A. Bunde, and W. Dieterich, *in* "Proceedings, of 6th International Symposium on Metals and Materials Science" (F. W. Poulsen *et al*., Eds.). Riso National Laboratory, Roskilde. (1985).
87. S. Bhandari, B. Tech thesis, IIT Bombay, 1998.